Research article

LUMINESCENCE
The Journal of Biological and Chemical Luminescence

Received: 09 September 2015, Revised: 23 November 2015, Accepted: 25 January 2016 Published online in Wiley Online Library

(wileyonlinelibrary.com) DOI 10.1002/bio.3118

Micro-photoluminescence of single living diatom cells

Paul LeDuff,[a] Guritno Roesijadi[b] and Gregory L. Rorrer[a]*

ABSTRACT: Diatoms are single-celled microalgae that possess a nanostructured, porous biosilica shell called a frustule. This study characterized the micro-photoluminescence (μ-PL) emission of single living cells of the photosynthetic marine diatom *Thalassiosira pseudonana* in response to UV laser irradiation at 325 nm using a confocal Raman microscope. The photoluminescence (PL) spectrum had two primary peaks, one centered at 500–510 nm, which was attributed to the frustule biosilica, and a second peak at 680 nm, which was attributed to auto-fluorescence of photosynthetic pigments. The portion of the μ-PL emission spectrum associated with biosilica frustule in the single living diatom cell was similar to that from single biosilica frustules isolated from these diatom cells. The PL emission by the biosilica frustule in the living cell emerged only after cells were cultivated to silicon depletion. The discovery of the discovery of PL emission by the frustule biosilica within a single living diatom itself, not just its isolated frustule, opens up future possibilities for living biosensor applications, where the interaction of diatom cells with other molecules can be probed by μ-PL spectroscopy. Copyright © 2016 John Wiley & Sons, Ltd.

Keywords: biosilica; diatom; photoluminescence

Introduction

Nature is an inspirational source of biologically derived silica structures with unique optical properties. In particular, diatoms are a prolific class of single-celled algae that possess silica shells or 'frustules' with intricate submicron and nanoscale features which have unique photonic (1) and optoelectronic (2) properties. During frustule development, membrane-bound transporters actively take up the soluble silicon in the form of silicic acid (3). Once inside the cell, silicic acid is converted into silica and molded into nanostructures by protein-mediated condensation reactions within the silicon deposition vesicle (4).

Nanostructured biosilica from cultured photosynthetic diatom cells has shown to possess photoluminescencent (PL) properties, exhibiting strong blue light emission upon UV excitation (5,6). Furthermore, cultivation of diatom cells under controlled delivery of soluble silicon and other trace metals offers a route to make nanostructured diatom silica with controlled PL and electroluminescent properties (7,8). The PL properties of diatom biosilica have been harnessed for sensing and biosensing applications (9–11).

In our previous work (5), frustule biosilica isolated from cultured diatom cells by hydrogen peroxide treatment had exhibited PL emission centered around 440–500 nm under UV excitation at 337 nm. The cultivation state also strongly affected the PL response, with frustules isolated from stationary phase cells at silicon depletion showing the highest PL emission. In this study, we measure the PL properties of single living diatom cells from the model photosynthetic marine diatom *Thalassiosira pseudonana*. We show that single living diatom cells exhibit photoluminescent behavior, and that the portion of the PL emission spectrum attributed to diatom biosilica emerges only after the cells are cultivated to silicon depletion.

Experimental

Diatom cell culture

Axenic cultures of the photosynthetic marine diatom *T. pseudonana* were obtained from UTEX The Culture Collection of Algae (UTEX # LB FD2) and cultivated in foam-stoppered 500 mL (VWR, Radnor, PA) flasks with 100 mL of Harrison's Artificial Seawater Medium enriched with f/2 nutrients and 0.50 mM dissolved silicon as Na_2SiO_3 as described previously (12). Flask cultures were maintained at 22°C and 21 $\mu E/m^2$-s incident light intensity on a 14 h light/10 h dark photoperiod, on an orbital shaker at 100 rpm. The cell suspension was subcultured at 10% v/v every 14 days.

In the flask culture cultivation experiment, the cell suspension was inoculated to an initial cell density of 1.8×10^6 cells/mL, and 5.0 mL samples were removed from the flask every 24 h and assayed for cell number density and dissolved silicon concentration. For cell number density, a 0.1 mL aliquot of the cell suspension was diluted in 10.0 mL of saline electrolyte solution and counted on a Beckman Z2 Coulter Counter (Beckman Coulter, Brea, CA) at a minimum threshold of 4 μm. Triplicate cell counts were performed on each sample. Immediately following the cell count, the cell suspension was filtered with a 0.45 μm Polytetrafluoroethylene (PTFE) syringe filter to separate the cell mass from the supernatant. The dissolved silicon concentration

* Correspondence to: G. L. Rorrer, School of Chemical, Biological, and Environmental Engineering, Oregon State University, Corvallis, OR 97331, USA. E-mail: rorrergl@engr.orst.edu

[a] School of Chemical, Biological, and Environmental Engineering, Oregon State University, Corvallis, OR 97331, USA

[b] Department of Microbiology, Oregon State University, Corvallis, OR 97331, USA

in the supernatant was determined by spectrophotometric assay at 360 nm following derivatization of 1.0 mL of cell culture supernatant (diluted to 5.0 mL with silicon-free distilled H_2O) with 0.2 mL 13.3% w/v ammonium molybdate reagent in water and 0.1 mL 13.7% v/v HCl in distilled water (13). Duplicate assays were performed on each sample.

PL of single living diatom cells and single biosilica frustules

Single diatom cells from the flask cultivation experiment were analyzed by micro-photoluminescence (μ-PL) spectroscopy. Living cells were deposited on a clean silicon surface so that the biosilica signal from the diatom frustule within the cell could be resolved. A square silicon wafer (1.0 cm/side) was cleaned with 70% v/v ethanol, dried under sterile air, and placed within a Petri dish containing a damp paper towel. A 5 μL aliquot of diatom cell suspension (~ 1×10^5 cells/mL) was pipetted onto the cleaned silicon wafer, where the droplet dispersed to nominal diameter of 5 mm, with the cells also dispersed as a monolayer on the wafer surface. The cells were kept hydrated in the humidified petri dish and immediately analyzed by μ-PL. Biosilica frustules were soaked in fresh culture medium and treated similarly prior to μ-PL analysis.

The μ-PL measurements on a single living cell were performed on a Horiba Jobin Yvon Lab (Horiba Jobin Yvon, Edison, New Jersey) Ram HR confocal Raman microscope equipped with a Kimmon 325 nm (Kimmon Electric, Centennial, CO) He–Cd laser (IK3151R-E, 15 mW average power), as shown in Fig. 1. A single cell on the silicon wafer in the valve up orientation was imaged under a ×40 UV objective of the Olympus BS41 microscope with a 400 μm field of view. The laser spot diameter was determined by 1.22 λ/NA, where λ is the laser wavelength (nm) and NA is the numerical aperture. At ×40 magnification, NA was set to 0.5, and the laser spot diameter at λ = 325 nm was 0.8 μm. The laser spot was manually targeted to the center of the cell. The cell was individually lased at times of 0, 20 and 40 s before emission spectra collection. At the end of each lasing time, the emitted light was passed through the ×40 UV objective with D1 optical density filter, and the filtered PL spectra were captured by a Synapse CCD (Horiba Jobin Yvon, Edison, New Jersey) detector (model 354308, 300 grating) with an integration time of 3 s. The process was repeated for five individual cells. All spectra were corrected for the silicon wafer background.

Frustule isolation

Intact frustules of T. *pseudonana* cells were isolated by detergent extraction and by hydrogen peroxide treatment. For detergent treatment, centrifuged cells were re-suspended in 0.5 mL of 100 mM EDTA containing 1% of the non-ionic detergent IGEPAL CA-630 [octylphenoxy poly(ethyleneoxy)ethanol, Sigma-Aldrich (Sigma-Aldrich, St. Louis, MO) 18896], vortexed, and extracted at 37°C for 60 min under gentle continuous shaking (~ 10^7–10^8 cells per 1.0 mL Eppendorf tube). The treated cells were microcentrifuged (13,200 ***g*** for 5 min) and the pellet was re-extracted for 5 min the same conditions three times. The final white product was washed/centrifuged in 1.0 mL double-distilled water three times, once in 1.0 mL of phosphate buffer B (20 mM sodium phosphate, 100 mM EDTA, pH 7.0), and then stored in 0.1 mL phosphate buffer. Frustules were also isolated from diatom cells by treatment with 30 wt% aqueous hydrogen peroxide at pH 2.5, as described previously (9).

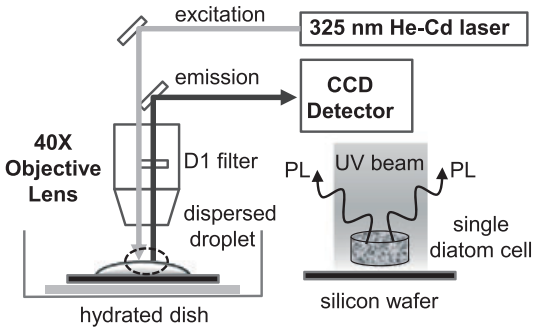

Figure 1. Setup for μ-PL measurements of a single diatom cell using the Raman microscope (not to scale).

Scanning electron microscopy of diatom cells

Whole cells were imaged by scanning electron microscopy (SEM) after fixation with glutaraldehyde and critical point drying. To prepare the sample, one drop of diatom cell suspension from the flask cultivation was allowed to gravity settle on to a clean 5 × 7 mm silicon wafer for 30 min at 20°C. The adhered cells were then fixed in 2.5 wt% glutaraldehyde and 1 wt% paraform in 0.1 M sodium cacodylate buffer for 30 min at 20°C. The fixative was washed off with 0.1 M cacodylate buffer for 10 min, and the cells were then dehydrated by an ethanol series (10% to 100% in 20–30% increments) for 10 min each at 20°C. The dehydrated samples were dried in a critical point dryer and then gold sputtered before analysis on a FEI Quanta 600 FEG SEM (FEI Company, Hillsboro, OR). The physical dimensions of 14 randomly selected diatom cells were determined by image analysis of their SEM images. The nominal thickness of the diatom frustule (t) was estimated by

$$t = \frac{m_{SiO2}\left(V_{pore} + 1/\rho_{SiO2}\right)}{\pi d(l + 0.5d)}$$

where d is the valve diameter, l is the girdle band length, ρ_{SiO2} the density of silica (2.2 g/cm^3), V_{pore} is the diatom frustule macropore volume [2.2 cm^3/g, taken from Liu et al. (14)] and m_{SiO2} is the amount of SiO_2 per cell (g/cell), estimated from the Si consumed per cell at the stationary phase of growth.

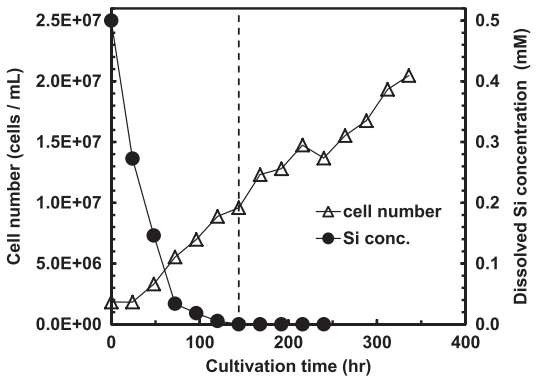

Figure 2. Cell number density and dissolved silicon concentration vs. time profiles for the flask-cultured *T. pseudonana* diatom cell suspension. The dotted line indicates the boundary at silicon limitation.

LUMINESCENCE
The Journal of Biological and Chemical Luminescence

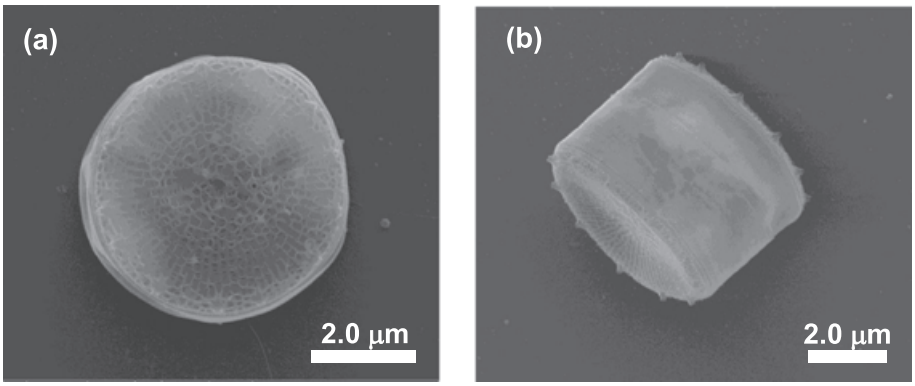

Figure 3. SEM images of whole *T. pseudonana* diatom cells after critical point drying. (a) Valve up view; (b) girdle band view.

Results and discussion

The cell number density and dissolved silicon concentration vs. time profiles for the flask-cultured *T. pseudonana* cell suspension are presented in Fig. 2. Silicon starvation was achieved after 144 h. After this time, one more nominal cell division occurred to achieve a final cell number density of 2.0×10^6 cells/mL after 336 h, and an estimated silica content of 1.6 pg/cell (nominally 3.5 wt % biosilica in living cell). SEM images of whole *T. pseudonana* diatom cells after 336 h of cultivation, prepared by critical point drying are provided in Fig. 3. The biosilica frustule structure is clearly evident. The average dimensions of the diatom cells are provided in Table 1. The frustule thickness was estimated to be 67 nm, consistent with previous measurements of frustule thickness for *T. pseudonana*, which varied from 52 to 80 nm (15).

The μ-PL spectrum of the living diatom cells after 72 and 312 h cultivation time are compared in Fig. 4. In these measurements, the lasing time was 40 s. There are two primary peaks, one centered at ~ 500–510 nm, and a second larger peak centered at ~ 680 nm. The peak at 500 nm is attributed to the biosilica in the diatom frustule of the living cell. The peak at 680 nm is attributed to auto-fluorescence of photosynthetic pigments in diatom cells (16). For cells cultivated at 72 h in the active stage of silicon-replete growth, the emission in the 500 nm range was clearly present but very weak (see Fig. 4, inset). However, for cells cultivated at 312 h, where silicon starvation was achieved and the cells were moving towards stationary phase, the PL emission spectra in the 450–600 nm range strongly emerged with peak wavelength centered at 500–510 nm.

The average PL peak emission (500–510 nm) for single living diatom cells vs. cultivation time is presented in Fig. 5. The PL response was normalized to the measurement at 24 h to more readily resolve relative changes during cell suspension growth. The peak PL emission decreased from the inoculum state during active cell division and silicon consumption, decreasing to almost zero just before the onset of silicon starvation. However, after silicon starvation was achieved and the cell culture moved towards stationary phase, the PL emission increased dramatically and then leveled off. Errors in the mean PL measurements were due to variabilities associated with the single cell measurement technique, including placement of the laser line on the cell and time-dependent PL response of the lasing time.

Table 1. *T. pseudonana* dimensions from SEM measurements

Frustule dimension	Average	1.0 SD (n = 14)
Mean valve diameter (μm)	4.3	± 0.9
Mean girdle band length (μm)	3.3	± 0.6
Mean outer surface area (μm^2)	74	± 27
Estimated frustule thickness (nm)	67	± 24

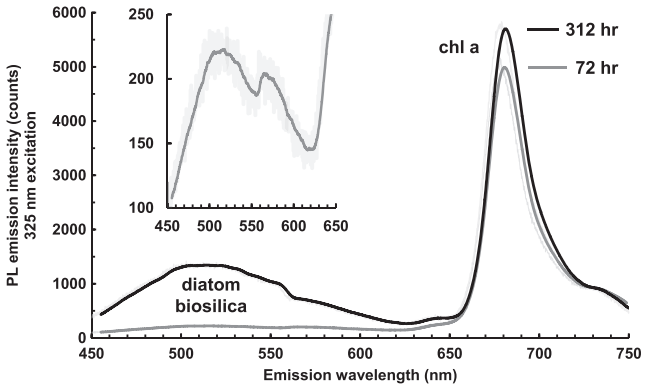

Figure 4. Representative μ-PL spectrum of *T. pseudonana* living diatom cells at 72 and 312 h cultivation time. Lasing time was 40 s. (Inset) The μ-PL spectrum at 72 h with scale adjusted to reveal spectrum peak in the 450–650 nm range.

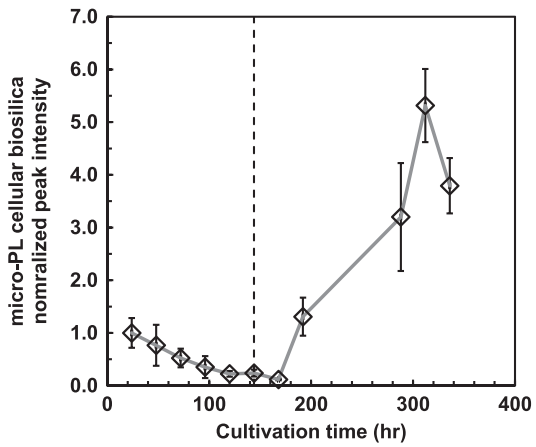

Figure 5. Average μ-PL peak emission (500–510 nm) of *T. pseudonana* living diatom cells vs. cultivation time. Error bars are ± 1.0 standard error based on 15 pooled measurements per cultivation time. The dotted line indicates the boundary at silicon limitation.

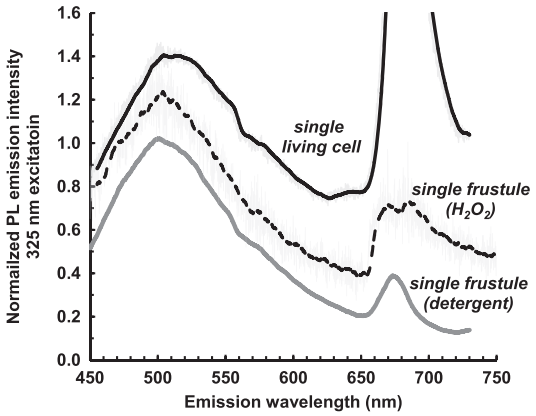

Figure 6. Comparison of representative μ-PL spectrum of a single living *T. pseudonana* diatom cell and single intact diatom frustule isolated by detergent and H_2O_2 treatments after 336 h cultivation, with focus on the biosilica peak range, at a lasing time of 40 s. Each PL signal was normalized to peak biosilica signal, and then offset to stack the spectra.

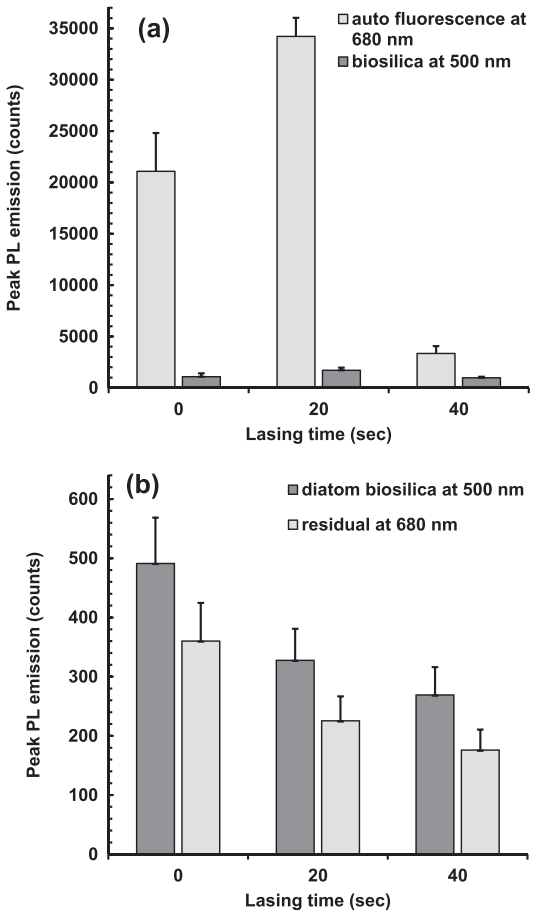

Figure 7. Effects of lasing time on μ-PL peak response for biosilica (500 nm) and chlorophyll auto-fluorescence (680 nm) from single living *T. pseudonana* diatom cells (a) and vs. a single intact diatom frustule isolated by detergent treatment (b).

Representative μ-PL spectra from a single living cell and a single intact biosilica frustule isolated from the diatom cell are compared in Fig. 6. The biosilica peak was nominally the same for both the living diatom cell and its isolated diatom frustule, although for the diatom frustule the shoulder was narrower and the wavelength at peak emission was slightly lower (500 vs. 500–510 nm). The isolation of the frustule from the living diatom cell by the detergent extraction method was carried out under conditions designed to be minimally invasive to the native biosilica in the cell. However, there was still residual organic material in the frustule, as evidenced by the small chlorophyll auto-fluorescence peak at 680 nm. Frustules isolated using the harsher hydrogen peroxide treatment method also possessed a residual peak at 680 nm. The likely sources of PL emission by diatom biosilica under UV excitation have been detailed in our previous work (5,7–9), where silanol groups (Si-OH) on nanostructured silica were largely responsible for PL emission in the 450–500 nm range, consistent with a radiative decay mechanism (17).

For the living diatom cell, increasing the lasing time for the PL analysis significantly decreased the emission peak centered at 680 nm, but only modestly decreased the peak centered at 500 nm (Fig. 7). Most likely, the increased lasing time decomposed the photosynthetic pigments, leading to a decrease in the auto-fluorescence signal intensity. The cell viability after the μ-PL analysis was not tested, but it was assumed that lasing action after 40 s rendered the cell nonviable.

The model diatom described in this study, *T. pseudonana*, is nominally 4 μm in diameter. However, large centric diatoms with nominal diameters of 200 μm that possess intricate pore arrays, such *Coscinodiscus* species, exhibit interesting optical properties when exposed to visible laser light, including light confinement (18,19), optical diffraction (20), and wavelength-dependent lens behavior (21,22).

Conclusions

This study showed for the first time that the biosilica frustules inside living diatom cells can exhibit PL emission in response to UV excitation. Furthermore, we showed that PL emission by the biosilica frustule within the living cell emerged only after cells were cultivated to silicon depletion. The portion of the μ-PL emission spectrum associated with biosilica frustule in the single living diatom cell was similar to that from single biosilica frustules isolated from these diatom cells. The emergence of the PL signal for the biosilica frustule was attributed to the likely formation of nanoscale fine features on the frustule following silicon depletion from the medium, as first identified by Qin et al. (5) for frustules isolated by diatom cell cultivation at various points in the cell cycle.

In this study, the discovery of PL emission by the biosilica frustule in living diatom cells opens up future possibilities for living biosensor applications, where the interaction of diatom cells with other molecules can be probed by μ-PL spectroscopy. In previous work (9), we showed diatom biosilica functionalized with antibodies showed enhancement of PL response upon immunocomplex formation, due to electron donor groups on antibody and the immunocomplex. Likewise, enzymes and antibodies can now be expressed directly on the biosilica itself during frustule biosynthesis, using recently developed genetic engineering techniques with *T. pseudonana* as the model organism (23–25). It may now be possible to interrogate the attachment of foreign antibodies expressed on diatom biosilica of living cells and their interaction with other molecules through μ-PL.

Acknowledgements

Support of this research was provided by U.S. Office of Naval Research, Synthetic Biology Program, Award Number N00014-12-1-0313 to Oregon State University.

LUMINESCENCE
The Journal of Biological and Chemical Luminescence

References

1. De Stefano L, Maddalena P, Moretti L, Rea I, Rendina I, De Tommasi E, et al. Nano-biosilica from marine diatoms: a brand new material for photonic applications. Superlatt Microstruct 2009;46:84–9.
2. Jeffryes C, Campbell J, Li H, Jiao J, Rorrer GL. The potential of diatom nanobiotechnology for applications in solar cells, batteries, and electroluminescent devices. Energ Environ Sci 2011;4:3930–41.
3. Martin-Jezequel V, Hildebrand M, Brezinski MA. Silicon metabolism in diatoms: implications for growth. J Phycol 2000;36:821–40.
4. Sumper M, Brunner E. Learning from diatoms: nature's tools for the production of nanostructured silica. Adv Funct Mater 2006;16:17–26.
5. Qin T, Gutu T, Jiao J, Chang CH, Rorrer GL. Photoluminescence of silica nanostructures from bioreactor culture of marine diatom *Nitzschia frustulum*. J Nanosci Nanotechnol 2008;8:2392–8.
6. Arteaga-Larios NV, Nahmad Y, Navarro-Contreras HR, Encinas A, García-Mezaa JV. Photoluminescence shift in frustules of two pennate diatoms and nanostructural changes to their pores. Luminescence 2014;29:969–76.
7. Gale DK, Jeffryes C, Gutu T, Jiao J, Chang CH, Rorrer GL. Thermal annealing activates amplified photoluminescence of germanium metabolically doped in diatom biosilica. J Mater Chem 2011;21:10658–65.
8. Jeffryes C, Solanki R, Rangineni DH, Wang W, Chang CH, Rorrer GL. Electroluminescence and photoluminescence from nanostructured diatom frustules containing metabolically inserted germanium. Adv Mater 2008;20:2633–7.
9. Gale DK, Gutu T, Jiao J, Chang CH, Rorrer GL. Photoluminescence detection of biomolecules by antibody-functionalized diatom biosilica. Adv Funct Mater 2009;19:926–33.
10. Lettieri S, Setaro A, De Stefano L, De Stefano M, Maddalena P. The gas-detection properties of light-emitting diatoms. Adv Funct Mater 2008;18:1257–64.
11. De Stefano L, Rotiroti L, De Stefano M, Lamberti A, Lettieri S, Setaro A, et al. Marine diatoms as optical biosensors. Biosens Bioelectron 2009;24:1580–4.
12. Jeffryes C, Rosenburger J, Rorrer GL. Fed-batch cultivation and bioprocess modeling of *Cyclotella* sp. for enhanced fatty acid production by controlled silicon limitation. Algal Res 2013;2:16–27.
13. Fanning KA, Pilson MEQ. On the spectrophotometric determination of dissolved silica in natural waters. Anal Chem 1973;45:136–40.
14. Liu D, Yuan P, Tan D, Liu H, Wang T, Fan M, et al. Facile preparation of hierarchically porous carbon using diatomite as both template and catalyst and methylene blue adsorption of carbon products. J Colloid Interf Sci 2012;388:176–84.
15. Li G, Campbell DA. Rising CO_2 interacts with growth light and growth rate to alter Photosystem II photoinactivation of the coastal diatom *Thalassiosira pseudonana*. PLoS One 2013;8:e55562.
16. Orellana MV, Petersen TW, van den Engh G. UV-excited blue auto-fluorescence of *Pseudo-nitzschia multiseries* (Bacillariophyceae). J Phycol 2004;40:705–0.
17. Rückschloss M, Wirschem T, Tamura H, Ruhl G, Oswald J, Vepřek S. Photoluminescence from OH-related radiative centres in silica, metal oxides and oxidized nanocrystalline and porous silicon. J Lumin 1995;63:279–87.
18. Di Caprio G, Coppola G, De Stefano L, De Stefano M, Antonucci A, Congestri R, et al. Shedding light on diatom photonics by means of digital holography. J Biophotonics 2012;7:341–50.
19. Ferrara MA, Dardano P, De Stefano L, Rea I, Coppola G. Optical properties of diatom nanostructured biosilica in *Arachnoidiscus* sp: micro-optics from Mother Nature. PLoS One 2014;9:e103750.
20. Kieu K, Li C, Fang Y, Cohoon G, Herrera OD, Hildebrand M, et al. Structure-based optical filtering by the silica microshell of the centricmarine diatom *Coscinodiscus wailesii*. Opt Express 2014;22:15992–9.
21. Romann J, Valmalette JC, Røyset A, Einarsrud MA. Optical properties of single diatom frustules revealed by confocal microspectroscopy. Opt Lett 2015;40:740–3.
22. De Tommasi E, Rea I, Mocella V, Moretti L, De Stefano M, Rendina I, et al. Multi-wavelength study of light transmitted through a single marine centric diatom. Opt Express 2010;18:12203–12.
23. Kröger N, Brunner E. Complex-shaped microbial biominerals for nanotechnology. WIREs Nanomed Nanobiotechnol 2014;6:615–27.
24. Sheppard VC, Scheffel A, Poulsen N, Kröger N. Live diatom silica immobilization of multimeric and redox-active enzymes. Appl Environ Microbiol 2012;78:211–8.
25. Marshall KE, Robinson EW, Hengel SM, Paša-Tolić L, Roesijadi G. FRET imaging of diatoms expressing a biosilica-localized ribose sensor. PLoS One 2012;7:e33771.